Inorganic Chemistry

Article

pubs.acs.org/IC

Novel (3,4,6)-Connected Metal–Organic Framework with High Stability and Gas-Uptake Capability

Chao Hou, Qing Liu, Jian Fan, Yue Zhao, Peng Wang, and Wei-Yin Sun*

Coordination Chemistry Institute, State Key Laboratory of Coordination Chemistry, School of Chemistry and Chemical Engineering, Nanjing National Laboratory of Microstructures, Nanjing University, Nanjing 210093, China

Supporting Information

ABSTRACT: A microporous and noninterpenetrated metal–organic framework $[Cu_3(L)_2(DABCO)(H_2O)]\cdot 15H_2O\cdot 9DMF$ (**1**) has been synthesized using two different ligands, [1,1′:3′,1″-terphenyl]-4,4″,5′-tricarboxylic acid (H_3L) and 1,4-diazabicyclo[2.2.2]octane (DABCO). As revealed by variable-temperature powder X-ray diffraction (VT-PXRD) measurements, *N*,*N*′-ditopic DABCO plays an important role for stabilization of the Cu–L framework. The three-dimensional framework of **1** exhibits high stability and excellent adsorption capacity for H_2 (54.3 mg g^{-1} at 77 K and 20 bar), CO_2 (871 mg g^{-1} at 298 K and 20 bar), CH_4 (116.7 mg g^{-1}, 99 cm^3 (STP) cm^{-3} at 298 K and 20 bar), and *n*-pentane (686 mg g^{-1} at 298 K and 1 bar). Interestingly, the excellent selectivity toward CO_2 over N_2 at ambient temperature (273 and 298 K) and 1 bar makes complex **1** possess practical application in gas separation and purification.

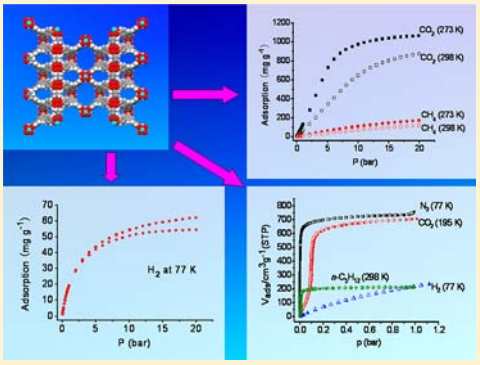

INTRODUCTION

Metal–organic frameworks (MOFs) with high stability, high surface area, and large pore volume have been attracting extensive interest in recent years not only because of their intriguing varieties of architectures and topologies[1] but also due to their potential applications in catalysis, gas storage/separation, and so on.[2] In order to achieve large pores within MOFs, a typical strategy is to increase the length of the bridging organic ligand.[2a,3] However, in some cases, long linkers lead to either collapse of the framework after removal of guest molecules or interpenetration of the framework which limits the pore size and volume.[4] It has been reported that the resultant framework could be stabilized by additional junction points through coordination of the secondary linker, and interpenetration could be effectively avoided by introducing a secondary linker to cross-link the initial framework.[5]

Thus far a large number of porous MOFs with expected structures and desired properties have been synthesized and reported through the rational design/selection of organic ligands and secondary building units (SBUs). Among the reported metal–carboxylate MOFs, the most well-known SBU is the paddle-wheel cluster $[M_2(OCO)_4]$ ($M = Cu^{2+}$, Zn^{2+}, Ni^{2+}), where the axial positions were occupied by solvent molecules or auxiliary ligands.[6] In considering the relatively strong coordination capability of pyridine and tertiary amine, the paddle-wheel cluster could be further linked by 4,4′-bipyridine (BPY) or 1,4-diazabicyclo[2.2.2]octane (DABCO).[7] As a secondary linker, DABCO shows an obvious advantage over BPY for construction of a noninterpenetrated framework because it is relatively short in length and bulky in width as compared with BPY.

Recently, Matzger and co-workers reported that a three-dimensional (3D) porous MOF, UMCM-151, was constructed by connection of $[Cu_2(OCO)_4]$ SBUs with [1,1′:3′,1″-terphenyl]-4,4″,5′-tricarboxylate (L^{3-}) ligand, which exhibits large channels but collapses after solvent removal, and afterward a smart strategy was applied to stabilize the overall framework by the increase of the ratio of benzene rings to carboxylate groups.[4b] Herein we use DABCO to overcome the problem of low structural rigidity of the Cu–L framework, and a new complex $[Cu_3(L)_2(DABCO)(H_2O)]\cdot 15H_2O\cdot 9DMF$ (**1**) was synthesized by reaction of H_3L, DABCO with copper(II) nitrate trihydrate under solvothermal conditions, which showed good stability up to 533 K after removal of lattice solvent molecules. Complex **1** is a 3D noninterpenetrated porous framework. Interestingly, complex **1** showed very good adsorption capacity for H_2 (54.3 mg g^{-1} at 77 K and 20 bar), CO_2 (871 mg g^{-1} at 298 K and 20 bar), CH_4 (116.7 mg g^{-1}, 99 cm^3 (STP) cm^{-3} at 298 K and 20 bar), and *n*-pentane (686 mg g^{-1} at 298 K and 1 bar). In addition, complex **1** exhibits excellent selectivity toward CO_2 over N_2 at ambient temperature.

EXPERIMENTAL SECTION

Materials and Measurements. All commercially available chemicals and solvents are of reagent grade and were used as received without further purification. The ligand H_3L was synthesized according to the literature.[4b] Elemental analyses for C, H, and N were performed on a Perkin-Elmer 240C Elemental Analyzer at the analysis center of Nanjing University. Thermogravimetric analyses (TGA) were

Received: May 9, 2012
Published: July 17, 2012

dx.doi.org/10.1021/ic300950h | *Inorg. Chem.* 2012, 51, 8402–8408

performed on a simultaneous SDT 2960 thermal analyzer under nitrogen with a heating rate of 10 K min^{-1}. FT-IR spectra were recorded in the range of 400−4000 cm^{-1} on a Bruker Vector22 FT-IR spectrophotometer using KBr pellets. Powder X-ray diffraction (PXRD) measurements were performed on a Bruker D8 Advance X-ray diffractometer using Cu Kα radiation (λ = 1.5418 Å), in which the X-ray tube was operated at 40 kV and 40 mA at room temperature.

Synthesis of [Cu_3(L)$_2$(DABCO)(H_2O)]·15H_2O·9DMF (1). A mixture of $Cu(NO_3)_2{\cdot}3H_2O$ (72.4 mg, 3 mmol), H_3L (72.5 mg, 2 mmol), DABCO (22.4 mg, 2 mmol), concentrated hydrochloric acid (150 μL), DMF (8 mL), dioxane (2 mL), and H_2O (2 mL) was treated by ultrasonic vibration and then sealed into a Teflon-lined stainless steel container and heated at 358 K for 3 days. After cooling to room temperature, blue-green block crystals were obtained in 90% yield (based on H_3L). Anal. Calcd for $C_{75}H_{129}N_{11}O_{37}Cu_3$: C, 45.78; H, 6.61; N, 7.83. Found: C, 45.75; H, 6.54; N, 7.80. IR (KBr pellet, cm^{-1}): 3441 (s), 2361 (w), 1655(s), 1618 (s), 1397 (s), 1181 (w), 1122 (w), 1015(w), 859 (w), 777 (m), 752 (w), 668 (w).

X-ray Crystallography. Structural data of **1** were collected on a Bruker Smart Apex DUO CCD with graphite-monochromated Mo Kα radiation (λ = 0.71073 Å) at 173(2) K. The structure was solved by direct methods and refined with the full-matrix least-squares technique using the SHELXS-97 and SHELXL-97 programs, respectively.[8] Because the guest solvent molecules are highly disordered and impossible to refine using conventional discrete-atom models, the SQUEEZE subroutine of the PLATON software suite[9] was applied to remove the scattering from the highly disordered solvent molecules, and sets of solvent-free diffraction intensities were produced. The final formula was calculated from the SQUEEZE results, TGA, and elemental analysis. Non-hydrogen atoms were refined anisotropically. The large thermal parameters of C100 and C101 are caused by disorder of DABCO. All hydrogen atoms were generated geometrically except H10F, which was located directly, while those of coordinated water molecule could not be found. Details of the crystal parameters, data collection, and refinements for the complex are summarized in Table 1, and selected bond lengths and angles are listed in Table 2.

Sample Activation. Solvent-exchanged sample was prepared by immersing the as-synthesized sample in acetone for 3 days to remove the nonvolatile solvates, the solvent was decanted every 8 h, and fresh acetone was added. The completely activated sample (**1a**) was obtained by heating the solvent-exchanged sample at 423 K under a dynamic high vacuum for 20 h. During this time, the blue-green sample changed to a dark-blue color, indicating the presence of unsaturated Cu(II) sites. Similar color change upon activation was observed for other frameworks constructed from Cu(II)−paddle-wheel SBUs.[10]

Table 1. Crystal Data and Structure Refinements for Complex 1

empirical formula	$C_{75}H_{129}Cu_3N_{11}O_{37}$
fw	1967.52
cryst syst	tetragonal
space group	$I4_1/amd$
a (Å)	19.156(5)
b (Å)	19.156(5)
c (Å)	61.292(5)
T (K)	173(2)
V (Å^3)	22491(9)
Z	8
ρ_{calcd} (g·cm^{-3})	0.614
μ (mm^{-1})	0.590
F(000)	4232
data collected	39 709
independent data	5272
goodness-of-fit	1.113
$R_1{}^a$ ($I > 2\sigma(I)$)	0.0381
$wR_2{}^b$ ($I > 2\sigma(I)$)	0.1165

$^aR_1 = \Sigma||F_o| - |F_c||/\Sigma|F_o|$. $^bwR_2 = |\Sigma w(|F_o|^2 - |F_c|^2)|/\Sigma|w(F_o)^2|^{1/2}$, where $w = 1/[\sigma^2(F_o^2) + (aP)^2 + bP]$. $P = (F_o^2 + 2F_c^2)/3$.

Table 2. Selected Bond Lengths (Angstroms) and Angles (degrees) for Complex 1[a]

Cu1−O1	1.9566(14)	Cu1−N1	2.186(2)
Cu1−O2#1	1.9562(14)	Cu2−O3	1.9460(16)
Cu2−O4	2.152(3)		
O2#1−Cu1−O2#2	87.70(10)	O2#1−Cu1−O1#3	167.64(6)
O1#3−Cu1−O1	88.68(10)	O2#1−Cu1−O1	90.49(7)
O2#1−Cu1−N1	97.26(6)	O1−Cu1−N1	95.10(6)
O3#4−Cu2−O3	168.56(9)	O3−Cu2−O3#6	89.91(10)
O3−Cu2−O3#5	88.95(10)	O3−Cu2−O4	95.72(4)

[a]Symmetry transformations used to generate equivalent atoms: #1 x, $-y + 1$, $-z + 1$; #2 $-x + 2$, $-y + 1$, $-z + 1$; #3 $-x + 2$, y, z; #4 $-x + 1$, $-y + 1/2$, z; #5 x, $-y + 1/2$, z; #6 $-x + 1$, y, z.

Sorption Measurements. In the gas sorption measurements, all of the gases used are of 99.999% purity. Low-pressure (up to 1 bar) nitrogen (N_2), carbon dioxide (CO_2), and *n*-pentane sorption experiments were carried out on a Belsorp-max volumetric gas sorption instrument. Low-pressure hydrogen (H_2) adsorption measurement (up to 1.1 bar) was performed on a Micromeritics ASAP 2020 M+C surface area analyzer. High-pressure adsorption isotherms of H_2 (at 77 K), CO_2 (at 273 and 298 K), and methane (CH_4, at 273 and 298 K) were measured using an IGA-003 gravimetric adsorption instrument (Hiden-Isochema, U.K.) over a pressure range of 0−20 bar. For high-pressure measurements, the completely activated sample mass was monitored until equilibrium was reached (within 25 min) at each pressure.

RESULTS AND DISCUSSION

Compound **1** was readily synthesized by solvothermal reaction of H_3L, DABCO, and $Cu(NO_3)_2{\cdot}3H_2O$ in a DMF−dioxane−H_2O solvent system. Single-crystal X-ray structural analysis revealed that **1** crystallizes in tetragonal system space group $I4_1/amd$. The asymmetric unit of **1** consists of one-half L^{3-}, one-quarter DABCO ligand, one-quarter coordinated H_2O molecule, and two crystallographically independent Cu(II) atoms both sitting on specific positions with one of one-half occupancy and the other one of one-quarter occupancy. As shown in Figure 1a, the Cu1 atom adopts a square pyramidal coordination geometry by four carboxylate O atoms from four different L^{3-} ligands and one N atom from a DABCO ligand. The two adjacent Cu1 atoms are linked together by four carboxylate groups to generate a paddle-wheel $[Cu_2(OCO)_4]$ subunit with a Cu···Cu separation of 2.6476(9) Å. The two axial sites of such a paddle-wheel subunit are occupied by two different DABCO ligands with the Cu−N bond length of 2.186(2) Å (Table 2), while in the paddle-wheel $[Cu_2(OCO)_4]$ subunit constructed by two Cu2 atoms the axial positions are occupied by coordinated water molecules with the Cu−O bond distance of 2.152(3) Å. The adjacent $[Cu_2(OCO)_4]$ subunits based on Cu1 atoms are connected by DABCO ligands to form infinite one-dimensional (1D) chain structure along both *a* and *b* axes (Figure 1b), which may be one cause for stabilization of complex **1**. The two kinds of Cu(II)−paddle-wheel subunits are connected by L^{3-} ligands and DABCO ligands to form a noninterpenetrated 3D framework with a large cavity (Figure 1c and 1d). A view along the *a* axis reveals large hexagonal-shaped channels with dimensions, accounting for van der Waals radii, of 19.2 Å × 15.3 Å formed through connection of four *p*-benzoate groups and four *m*-carboxylate groups coordinated through four Cu−paddlewheels. The total solvent cavity

dx.doi.org/10.1021/ic300950h | Inorg. Chem. 2012, 51, 8402−8408

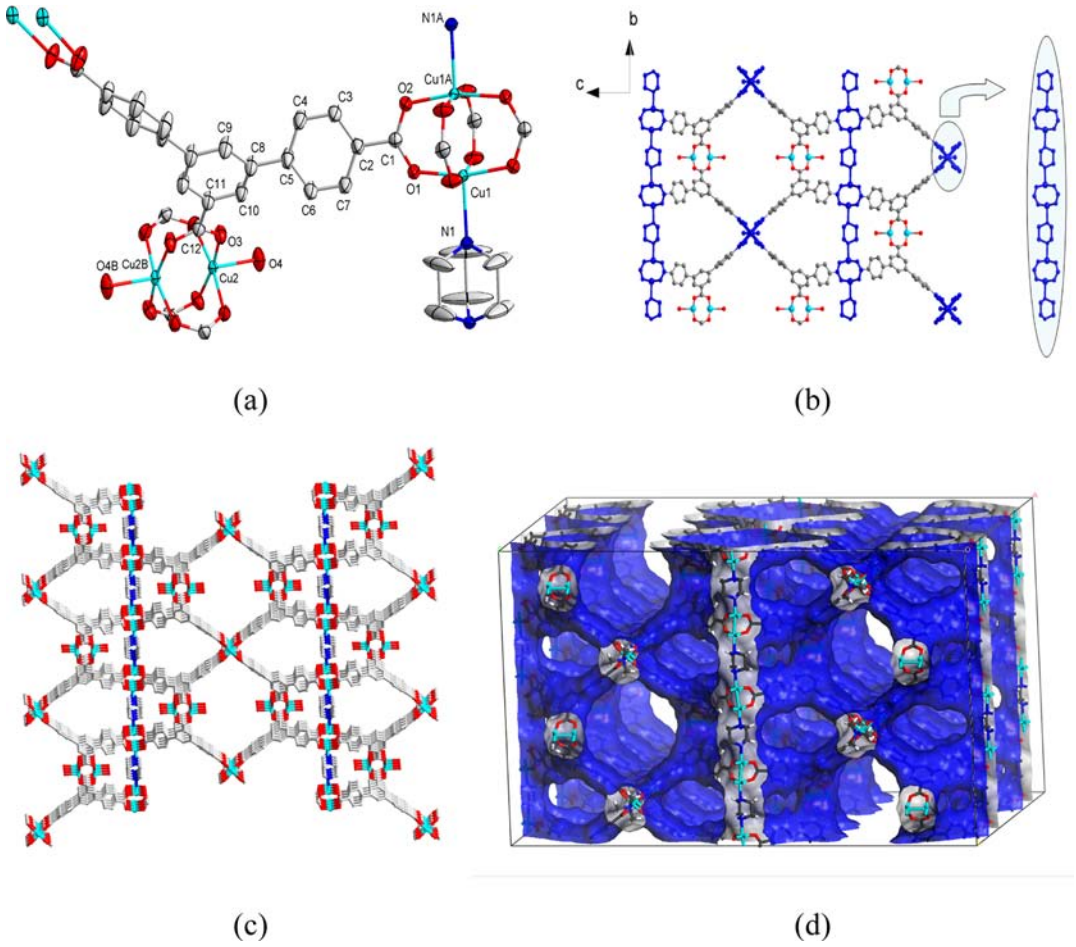

Figure 1. (a) Coordination environment of Cu(II) in **1** with ellipsoids drawn at the 30% probability level. Hydrogen atoms are omitted for clarity. (b) 1D chains formed by Cu1 paddle-wheel subunits and DABCO ligands viewed along *a* and *b* axes. Blue color represents the chains. (c) 3D structure of **1** with large cavity. (d) Connolly surface of **1a** with a probe radius of 1.4 Å showing the large three-dimensional cross-linking tunnels (inner surfaces, blue; outer surfaces, gray).

volume in **1** is 71.4% (16229 Å^3) per unit cell calculated by PLATON,[11] where all the solvents, including the coordinated water molecules, were excluded from the framework for the solvent cavity volume calculation.

To further understand the structure of **1**, topological analysis by reducing multidimensional structure to a simple node-and-linker net was performed. On the basis of the simplification principle,[12] each L^{3-} ligand connects three paddle-wheel SBUs and is considered as 3-connected node while the DABCO ligand acts as a 2-connector. Each Cu1−paddle-wheel SBU connects four L^{3-} ligands and two DABCO ligands and thus can be regarded as a 6-connector. Similarly, each Cu2−paddle-wheel SBU links four L^{3-} ligands and acts as a 4-connected node. Hence, the overall structure of **1** is a (3,4,6)-connected 3-nodal 3D net with stoichiometry $(3\text{-c})_4(4\text{-c})(6\text{-c})_2$, as shown in Figure 2. Topological analysis using TOPOS software[13] identified that the structure of **1** is a new topological net, which can be presented by a Schläfli symbol of $(5^{10}.8^5)_2(5^3)_4(5^4.8^2)$ (td10 = 1828).

The bulk identity and thermal stability of **1** were investigated by powder X-ray diffraction (PXRD) measurements and thermogravimetric analysis (TGA). The TGA curve (Figure S1, Supporting Information) of **1** reveals a weight loss of 13.76% in the temperature range of 298−371 K, which corresponds to loss of free H_2O molecules (calcd 13.74%).

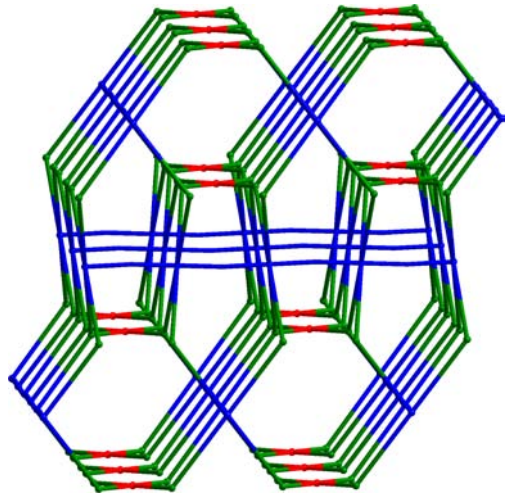

Figure 2. Schematic representation of the (3,4,6)-connected 3-nodal 3D network of **1** with $(5^{10}.8^5)_2(5^3)_4(5^4.8^2)$ topology: blue, Cu1; red, Cu2; green, L^{3-} ligands.

Another weight loss (34.27%) in the temperature range of 371−518 K is attributed to release of the coordinated H_2O and free DMF molecules (calcd 34.35%), and further weight losses were observed owing to decomposition of the framework.

dx.doi.org/10.1021/ic300950h | *Inorg. Chem.* 2012, 51, 8402−8408

Samples after solvent exchange and vacuum activation show similar weight loss curves (Figure S1, Supporting Information), which indicated the good stability of the framework after removal of solvent molecules. The similarity of simulated PXRD pattern from single-crystal data of **1** with that for as-synthesized sample **1** and for activated sample **1a** indicates that the single crystal is representative of the bulk sample, and the activated sample retained the same structure as that of **1** (Figure 3). The thermal stability of **1** has been demonstrated

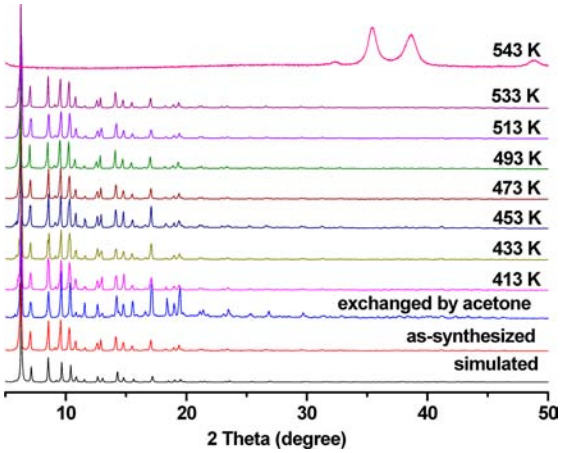

Figure 3. Variable-temperature PXRD patterns for **1**. Simulated pattern was calculated based upon the single-crystal structure.

using variable-temperature PXRD (VT-PXRD) experiments (Figure 3). The VT-PXRD patterns of as-synthesized sample show that the framework is stable at least up to 533 K, which is consistent with thermogravimetric analysis. Furthermore, sample **1** is stable in open air even after months (Figure 4b). The PXRD pattern of sample **1**, which was immersed in water overnight and dried at ambient temperature, showed loss of crystallinity (Figure 4c). However, after further soaked in DMF overnight, the sample completely recovered its crystallinity (Figure 4d). The activated sample **1a** shows the similar

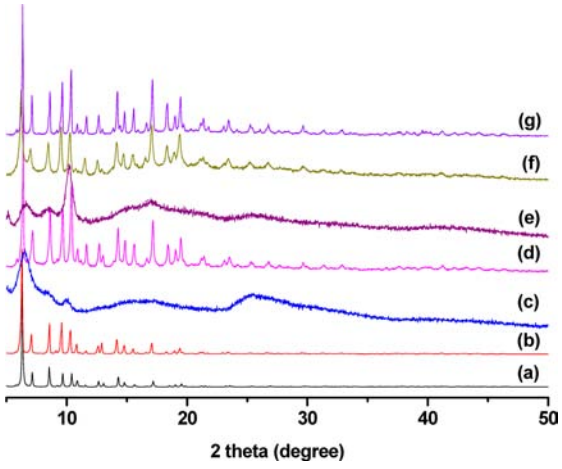

Figure 4. PXRD patterns under varied conditions: (a) simulated pattern; (b) exposed **1** in air for 3 months; (c) immersed **1** in water overnight; (d) prepared by soaking **1** in water overnight, in DMF overnight; (e) immersed **1a** in water overnight; (f) prepared by soaking **1a** in water overnight, in DMF overnight; (g) prepared by soaking **1a** in water overnight, in DMF overnight, then reactivated.

structural interconversion as complex **1** (Figure 4e–g), more importantly, the adsorption ability is almost the same before and after reformation, as illustrated by CO_2 sorption at 273 and 298 K and 1 bar (Figure S2, Supporting Information).

The high porosity and thermal stability make **1a** a good candidate for gas storage. To check the permanent porosity of **1a**, N_2 sorption isotherm at 77 K was measured, which showed type **I** adsorption behavior (Figure S3, Supporting Information). On the basis of the N_2 adsorption isotherm, the BET surface area of **1a** is estimated to be 2703 $m^2\ g^{-1}$ (Langmuir surface area 3154 $m^2\ g^{-1}$, Figure S4, Supporting Information), which is comparable to the values reported for other MOFs, such as MFU-4*l* (2750 $m^2\ g^{-1}$), SNU-6 (2590 $m^2\ g^{-1}$), and PCN-46 (2500 $m^2\ g^{-1}$).[14,15a] The pore volume obtained from the sorption isotherm at P = 0.9 bar is 1.13 $cm^3\ g^{-1}$, which is close to the value expected from the crystallographic data (1.18 $cm^3\ g^{-1}$). The pore-size distributions derived from the N_2 isotherms by the Horvath–Kawazoe (HK) method suggest that the average pore size for **1a** is 16.6 Å in diameter, which is consistent with the value expected from the crystallographic data (ca. 17 Å).

The H_2 adsorption isotherms measured at 77 K show the high H_2 uptake capability of **1a** (Figure 5). It adsorbs up to 20.9

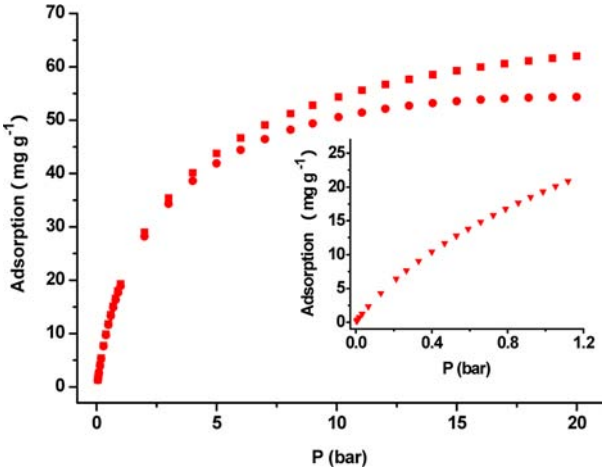

Figure 5. H_2 sorption isotherms for **1a** at 77 K and 0–20 bar, where filled squares and filled circles represent the total and excess H_2 sorption capacities, respectively. (Inset) H_2 sorption isotherm for **1a** at 77 K and 0–1.1 bar.

mg g^{-1} of H_2 (234 $cm^3\ g^{-1}$ at standard temperature and pressure (STP), 10.44 H_2 molecules per formula unit) at 77 K and 1.1 bar (Figure 5 inset). Values are comparable with those of previously reported Cu(II) MOFs that contain the accessible metal sites on Cu(II) paddle-wheels.[15,17,18] The high-pressure H_2 sorption study was performed using the gravimetric measurement method up to 20 bar. At 77 K, the excess and total gravimetric H_2 uptakes of **1a** reach 54.3 and 62.0 mg g^{-1}, respectively, which are lower than those of two reported MOFs for H_2 storage (NU-100,[16a] 99.5 and 164 mg g^{-1} at 56 bar; MOF-210,[16b] 86 and 176 mg g^{-1} at 80 bar) but comparable to those of PCN-46 (excess uptake, 56.1 mg g^{-1} at 32 bar),[15a] UMCM-1 (excess uptake, 57.5 mg g^{-1} at 45 bar),[17] SNU-50′ (excess uptake, 54.8 mg g^{-1} at 60 bar),[18a] and NOTT-103 (total uptake 65.1 mg g^{-1} at 20 bar).[18b]

The CO_2 adsorption isotherm of **1a** shows a CO_2 uptake capacity of 1382 mg g^{-1} (704 $cm^3\ g^{-1}$) at 195 K and 1 bar

dx.doi.org/10.1021/ic300950h | Inorg. Chem. 2012, 51, 8402–8408

(Figure 6). To the best of our knowledge, this CO_2 storage capacity at 195 K represents the third highest record so far

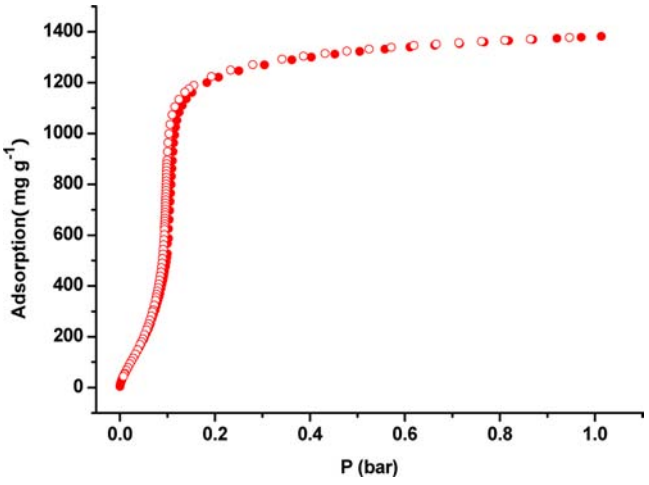

Figure 6. CO_2 adsorption isotherm for **1a** at 195 K, where filled shape and open shape represent adsorption and desorption, respectively.

reported for MOFs under similar conditions, which is just lower than that of Be-BDC[19] (1600 mg g^{-1}) and SNU-77H[20] (1688 mg g^{-1}) but greater than that of other reported MOFs such as SNU-6[14b] (1138 mg g^{-1}) and MCF-19[21] (1001 mg g^{-1}). Most interestingly, the CO_2 uptake of 120 mg g^{-1} (61.1 cm^3 g^{-1}, 10.7 wt %) at 273 K and 63 mg g^{-1} (32.0 cm^3 g^{-1}, 5.9 wt %) at 298 K is comparable to that for reported MOFs under the same conditions,[22] but almost no N_2 adsorption (8 mg g^{-1}, 6.1 cm^3 g^{-1} at 273 K and 5 mg g^{-1}, 3.8 cm^3 g^{-1} at 298 K) was observed for **1a** (Figure S2, Supporting Information). The selectivity ratio of CO_2 over N_2 is 12:1 at 0.1 bar (a typical partial pressure of CO_2 in industrial flue gas) and 10:1 at 1 bar.[23] The isosteric heat of CO_2 adsorption calculated using the virial method is 19.5 kJ mol^{-1} at low coverage range (Figure S5, Supporting Information). The value is higher than that for MOF-5 (15.6 kJ mol^{-1}) and MOF-508b (14.9 kJ mol^{-1}) but similar to that of UMCM-150 (20.6 kJ mol^{-1}) and UMCM-150(N)$_2$ (19.5 kJ mol^{-1}) also with open metal sites.[24] The high-pressure CO_2 adsorption isotherms are shown in Figure 7. **1a** adsorbs CO_2

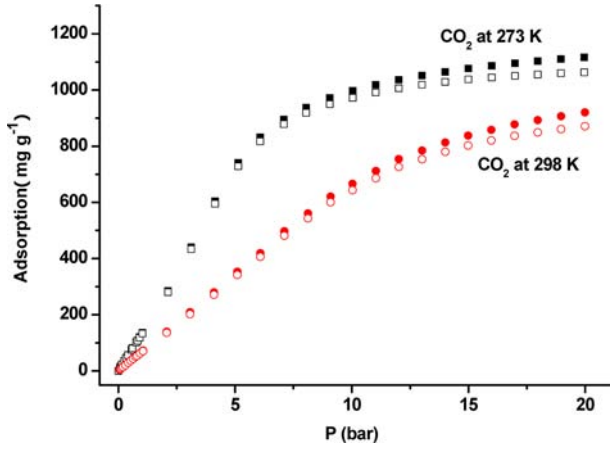

Figure 7. CO_2 sorption isotherms for **1a** at 0−20 bar, where squares and circles represent the isotherms at 273 and 298 K, respectively, and filled shape and open shape represent the total and excess CO_2 sorption capacities, respectively.

with an excess adsorption of 871 mg g^{-1} (19.8 mmol g^{-1}) and a total uptake of 920 mg g^{-1} at 298 K (1063 mg g^{-1}, 24.2 mmol g^{-1} and 1117 mg g^{-1} at 273 K) and 20 bar. In contrast to the reported MOFs with high CO_2 capture (e.g., MOF-210,[16b] 54.5 mmol g^{-1} at 50 bar; MOF-200,[16b] 55.4 mmol g^{-1} at 50 bar; NU-100,[16a] 46.4 mmol g^{-1} at 40 bar), **1a** still has relatively high uptake (PCN-46,[15a] 21.0 mmol g^{-1} at 30 bar; IRMOF-6,[25] 19.5 mmol g^{-1} at 35 bar; IRMOF-3,[25] 18.7 mmol g^{-1} at 35 bar).

To further monitor the general gas storage capacity and behavior of **1a**, gravimetric CH_4 adsorption isotherms were also recorded up to 20 bar at both 273 and 298 K (Figure 8). Both

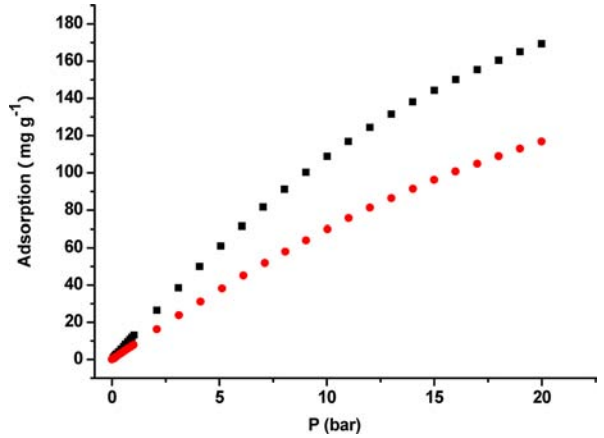

Figure 8. Excess CH_4 sorption isotherms at 0−20 bar, where squares and circles represent the isotherms at 273 and 298 K, respectively.

isotherms show typical type I behavior and fast kinetics. Restricted by the maximum pressure of the instrument here, we are unable to measure the sample at a higher pressure range. At 20 bar, the unsaturated CH_4 uptake of **1a** reaches 169.3 and 116.7 mg g^{-1} at 273 and 298 K, respectively, corresponding to volumetric (v/v) uptakes of 143 and 99 cm^3(STP) cm^{-3}, which is comparable to other MOF materials in higher pressure at 298 K (PCN-68,[15c] 99 cm^3(STP) cm^{-3} at 35 bar; NOTT-119a,[27] 97.8 cm^3(STP) cm^{-3} at 66 bar; DUT-13,[28] 71 cm^3(STP) cm^{-3} at 35 bar).

To gain insight into the adsorption capacity of **1a** for *n*-pentane, which is toxic to the environment, the adsorption isotherm was also collected (Figure 9). At 298 K and saturated vapor pressures, **1a** can adsorb *n*-pentane with a value of 686 mg g^{-1} (213 cm^3 g^{-1}) of the maximum amount, which indicates the excellent *n*-pentane storage capacity and affinity.[5b]

In summary, a 3D noninterpenetrating MOF, $[Cu_3(L)_2(DABCO)(H_2O)]\cdot 15H_2O\cdot 9DMF$ (**1**), is stabilized by the presence of secondary linker, DABCO. Sorption measurements of **1** revealed high storage capacities for H_2 (54.3 mg g^{-1} at 77 K and 20 bar), CO_2 (871 mg g^{-1} at 298 K and 20 bar), CH_4 (116.7 mg g^{-1}, 99 cm^3(STP) cm^{-3} at 298 K and 20 bar), and *n*-pentane (686 mg g^{-1}, 213 cm^3 g^{-1} at 298 K and 1 bar). Excellent CO_2/N_2 uptake ratios at ambient temperature (273 and 298 K) and 1 bar are revealed. The results indicate that replacement of coordinated solvent molecules on Cu−paddle-wheel SBUs with a *N,N′*-ditopic ligand not only enhanced the stability of the framework but also led to novel adsorption properties.

dx.doi.org/10.1021/ic300950h | *Inorg. Chem.* 2012, 51, 8402−8408

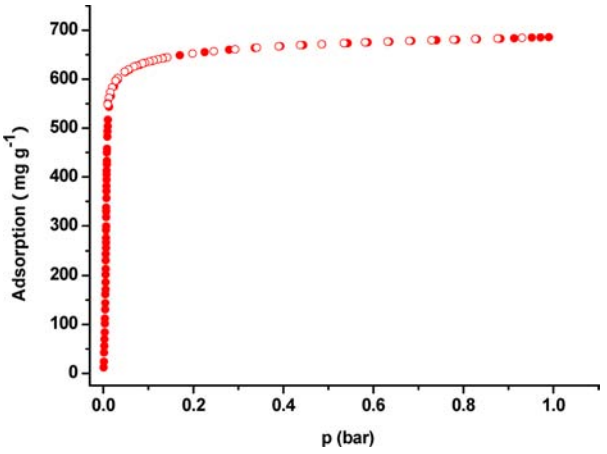

Figure 9. *n*-Pentane adsorption isotherm for **1a** at 298 K and 0−1 bar, where filled shape and open shape represent adsorption and desorption, respectively.

■ ASSOCIATED CONTENT

Ⓢ Supporting Information

X-ray crystallographic file in CIF format, TGA data, adsorption isotherms, and Q_{st} calculation details. This material is available free of charge via the Internet at http://pubs.acs.org.

■ AUTHOR INFORMATION

Corresponding Author

*E-mail: sunwy@nju.edu.cn.

Notes

The authors declare no competing financial interest.

■ ACKNOWLEDGMENTS

This work was financially supported by the National Basic Research Program of China (Grant no. 2010CB923303) and the National Natural Science Foundation of China (Grant nos. 91122001 and 21021062).

■ REFERENCES

(1) (a) Zheng, S.-T.; Bu, J. J.; Wu, T.; Chou, C.; Feng, P.; Bu, X. *Angew. Chem., Int. Ed.* **2011**, *50*, 8858. (b) Tranchemontagne, D. J.; Mendoza-Cortés, J. L.; O'Keeffe, M; Yaghi, O. M. *Chem. Soc. Rev.* **2009**, *38*, 1257. (c) Rosi, N. L.; Kim, J.; Eddaoudi, M.; Chen, B.; O'Keeffe, M; Yaghi, O. M. *J. Am. Chem. Soc.* **2005**, *127*, 1504.

(2) (a) Ma, L.; Falkowski, J. M.; Abney, C.; Lin, W. *Nat. Chem.* **2010**, *2*, 838. (b) Jeong, K. S.; Go, Y. B.; Shin, S. M.; Lee, S. J.; Kim, J.; Yaghi, O. M.; Jeong, N. *Chem. Sci.* **2011**, *2*, 877. (c) Murray, L. J.; Dincă, M.; Long, J. R. *Chem. Soc. Rev.* **2009**, *38*, 1294. (d) Ma, S.; Yuan, D.; Chang, J.-S.; Zhou, H.-C. *Inorg. Chem.* **2009**, *48*, 5398. (e) Li, J.-R.; Kuppler, R. J.; Zhou, H.-C. *Chem. Soc. Rev.* **2009**, *38*, 1477.

(3) (a) Eddaoudi, M.; Kim, J.; Rosi, N.; Vodak, D.; Wachter, J.; O'Keeffe, M.; Yaghi., O. M. *Science* **2002**, *295*, 469. (b) Lin, X.; Jia, J.; Zhao, X.; Thomas, K. M.; Blake, A. J.; Walker, G. S.; Champness, N. R.; Hubberstey, P.; Schröder, M. *Angew. Chem., Int. Ed.* **2006**, *45*, 7358.

(4) (a) Song, X.; Zou, Y.; Liu, X.; Oh, M.; Lah, M. S. *New J. Chem.* **2010**, *34*, 2396. (b) Schnobrich, J. K.; Lebel, O.; Cychosz, K. A.; Dailly, A.; Wong-Foy, A. G.; Matzger, A. J. *J. Am. Chem. Soc.* **2010**, *132*, 13941.

(5) (a) Kitaura, R.; Iwahori, F.; Matsuda, R.; Kitagawa, S.; Kubota, Y.; Takata, M.; Kobayashi, T. C. *Inorg. Chem.* **2004**, *43*, 6522. (b) Han, D.; Jiang, F.-L.; Wu, M.-Y.; Chen, L.; Chen, Q.-H.; Hong, M.-C. *Chem. Commun.* **2011**, *47*, 9861.

(6) (a) Chui, S. S.-Y.; S. Lo, M.-F.; Charmant, J. P. H.; Orpen, A. G.; Williams, I. D. *Science* **1999**, *283*, 1148. (b) He, Y.; Zhang, Z.; Xiang, S.; Fronczek, F. R.; Krishna, R.; Chen, B. *Chem.—Eur. J.* **2012**, *18*, 613. (c) Chen, B.; Eddaoudi, M.; Hyde, S. T.; O'Keeffe, M; Yaghi, O. M. *Science* **2001**, *291*, 1021. (d) Tan, C.; Yang, S.; Champness, N. R.; Lin, X.; Blake, A. J.; Lewis, W.; Schröder, M. *Chem. Commun.* **2011**, *47*, 4487. (e) Ma, S. Q.; Sun, D. F.; Simmons, J. M.; Collier, C. D.; Yuan, D. Q.; Zhou, H. C. *J. Am. Chem. Soc.* **2008**, *130*, 1012.

(7) (a) Zhang, P.; Li, B.; Zhao, Y.; Meng, X.; Zhang, T. *Chem. Commun.* **2011**, *47*, 7722. (b) Liu, X.; Oh, M.; Lah, M. S. *Inorg. Chem.* **2011**, *50*, 5044. (c) Eubank, J. F.; Wojtas, L.; Hight, M. R.; Bousquet, T.; Kravtsov, V. Ch.; Eddaoudi, M. *J. Am. Chem. Soc.* **2011**, *133*, 17532.

(8) (a) Sheldrick, G. M. *SHELXS97, program for crystal structure solution*; University of Göttingen: Göttingen, Germany, 1997. (b) Sheldrick, G. M. *SHELXL97, program for crystal structure refinement*; University of Göttingen: Göttingen, Germany, 1997.

(9) Spek, A. L. *Acta Crystallogr., Sect. A* **1990**, *46*, C34.

(10) (a) Chen, B.; Ockwig, N. W.; Millward, A. R.; Contreras, D. S.; Yaghi, O. M. *Angew. Chem., Int. Ed.* **2005**, *44*, 4745. (b) Yan, Y.; Lin, X.; Yang, S. H.; Blake, A. J.; Dailly, A.; Champness, N. R.; Hubberstey, P.; Schröder, M. *Chem. Commun.* **2009**, 1025. (c) Duan, J.; Yang, Z.; Bai, J.; Zheng, B.; Li, Y.; Li, S. *Chem. Commun.* **2012**, *48*, 3058.

(11) Spek, A. L. *J. Appl. Crystallogr.* **2003**, *36*, 7.

(12) Balaban, A. T. *From Chemical Topology to Three-Dimensional Geometry*; Plenum Press: New York, 1997.

(13) (a) Blatov, V. A. *IUCr CompComm Newslett.* **2006**, *7*, 4. (b) Blatov, V. A. *TOPOS, A Multipurpose Crystallochemical Analysis with the Program Package*; Samara State University: Russia, 2009.

(14) (a) Denysenko, D.; Grzywa, M.; Tonigold, M.; Streppel, B.; Krkljus, I.; Hirscher, M.; Mugnaioli, E.; Kolb, U.; Hanss, J.; Volkmer, D. *Chem.—Eur. J.* **2011**, *17*, 1837. (b) Park, H. J.; Suh, M. P. *Chem.—Eur. J* **2008**, *14*, 8812.

(15) (a) Zhao, D.; Yuan, D.; Yakovenko, A.; Zhou, H.-C. *Chem. Commun.* **2010**, *46*, 4196. (b) Yan, Y.; Telepeni, I.; Yang, S.; Lin, X.; Kockelmann, W.; Dailly, A.; Blake, A. J.; Lewis, W.; Walker, G. S.; Allan, D. R.; Barnett, S. A.; Champness, N. R.; Schröder, M. *J. Am. Chem. Soc.* **2010**, *132*, 4092. (c) Yuan, D.; Zhao, D.; Sun, D.; Zhou, H.-C. *Angew. Chem., Int. Ed.* **2010**, *49*, 5357.

(16) (a) Farha, O. K.; Yazaydin, A. O.; Eryazici, I.; Malliakas, C. D.; Hauser, B. G.; Kanatzidis, M. G.; Nguyen, S. T.; Snurr, R. Q.; Hupp, J. T. *Nat. Chem* **2010**, *2*, 944. (b) Furukawa, H.; Ko, N.; Go, Y. B.; Aratani, N.; Choi, S. B.; Choi, E.; Yazaydin, A. O.; Snurr, R. Q.; O'Keeffe, M.; Kim, J.; Yaghi, O. M. *Science* **2010**, *329*, 424.

(17) Wong-Foy, A. G.; Lebel, O.; Matzger, A. J. *J. Am. Chem. Soc.* **2007**, *129*, 15740.

(18) (a) Prasad, T. K.; Hong, D. H.; Suh, M. P. *Chem.—Eur. J.* **2010**, *16*, 14043. (b) Lin, X.; Telepeni, I.; Blake, A. J.; Dailly, A.; Brown, C. M.; Simmons, J. M.; Zoppi, M.; Walker, G. S.; Thomas, K. M.; Mays, T. J.; Hubberstey, P.; Champness, N. R.; Schröder, M. *J. Am. Chem. Soc.* **2009**, *131*, 2159.

(19) Porter, W. W.; Wong-Foy, A. G.; Dailly, A.; Matzger, A. J. *J. Mater. Chem.* **2009**, *19*, 6489.

(20) Park, H. J.; Lim, D.-W.; Yang, W. S.; Oh, T.-R.; Suh, M. P. *Chem.—Eur. J.* **2011**, *17*, 7251.

(21) Zhang, Y.-B.; Zhang, W.-X.; Feng, F.-Y.; Zhang, J.-P.; Chen, X.-M. *Angew. Chem., Int. Ed.* **2009**, *48*, 5287.

(22) Li, J.-R.; Ma, Y.; McCarthy, M. C.; Sculley, J.; Yu, J.; Jeong, H.-K.; Balbuena, P. B.; Zhou, H.-C. *Coord. Chem. Rev.* **2011**, *255*, 1791.

(23) (a) Caskey, S. R.; Wong-Foy, A. G.; Matzger, A. J. *J. Am. Chem. Soc.* **2008**, *130*, 10870. (b) Mason, J. A.; Sumida, K.; Herm, Z. R.; Krishna, R.; Long, J. R. *Energy Environ. Sci.* **2011**, *4*, 3030. (c) Choi, H.-S.; Suh, M. P. *Angew. Chem., Int. Ed.* **2009**, *48*, 6865. (d) Demessence, A.; D'Alessandro, D. M.; Foo, M. L.; Long, J. R. *J. Am. Chem. Soc.* **2009**, *131*, 8784. (e) Banerjee, R.; Furukawa, H.; Britt, D.; Knobler, C.; O'Keeffe, M.; Yaghi, O. M. *J. Am. Chem. Soc.* **2009**, *131*, 3875.

(24) (a) Babarao, R.; Jiang, J. *Langmuir* **2008**, *24*, 6270. (b) Bastin, L.; Bárcia, P. S.; Hurtado, E. J.; Silva, J. A. C.; Rodrigues, A. E.; Chen, B. *J. Phys. Chem. C* **2008**, *112*, 1575. (c) Yazaydin, A. Ö; Snurr, R. Q.; Park, T.-H.; Koh, K.; Liu, J.; Levan, M. D.; Benin, A. I.; Jakubczak, P.; Lanuza, M.; Galloway, D. B.; Low, J. J.; Wills, R. R. *J. Am. Chem. Soc.* **2009**, *131*, 18198.

(25) Millward, A. R.; Yaghi, O. M. *J. Am. Chem. Soc.* **2005**, *127*, 17998.
(26) Ma, S.; Sun, D.; Simmons, J. M.; Collier, C. D.; Yuan, D.; Zhou, H.-C. *J. Am. Chem. Soc.* **2008**, *130*, 1012.
(27) Yan, Y.; Yang, S.; Blake, A. J.; Lewis, W.; Poirier, E.; Barnett, S. A.; Champness, N. R.; Schröder, M. *Chem. Commun.* **2011**, *47*, 9995.
(28) Grünker, R.; Senkovska, I.; Biedermann, R.; Klein, N.; Lohe, M. R.; Müller, P.; Kaskel, S. *Chem. Commun.* **2011**, *47*, 490.